Advance Sustainable Science, Engineering and Technology (ASSET)
Vol. 8, No.1, January 2026, pp. 02601027-01 ~ 02601027-014
ISSN: 2715-4211 DOI: https://doi.org/10.26877/asset.v8i1.2566

# Risk-Based Zoning for Urban Flood Mitigation Using HEC-HMS–HEC-RAS 2D Areas

**Oktavia Kurnianingsih[1], Rr Rintis Hadiani[2*], Bambang Setiawan[2], Sobriyah[2]**

[1]Applied Bachelor of Construction Management, Vocational School, Sebelas Maret University, Jl. Ir. Sutami No. 36A, Surakarta City, Central Java 57121, Indonesia

[2]Department of Civil Engineering, Sebelas Maret University, Jl. Ir. Sutami No. 36A, Surakarta City, Central Java 57121, Indonesia

*rintis@ft.uns.ac.id

**Abstract**. This study aims to assess the potential for urban inundation and formulate flood mitigation strategies based on spatial analysis. A 2D modelling approach using HEC-HMS and HEC-RAS was applied to simulate the extent and depth of inundation in the urban area of Karanganyar, Indonesia. The models were validated with field observations using RMSE. Model validation confirmed the agreement between simulated and observed data. Validation was quantified using RMSE = 0.42 m across 15 checkpoints, with an average MAE of 0.31 m, and a coefficient of determination ($R^2$) of 0.87. The 2D mesh resolution was set at 10 m, balancing computational efficiency with spatial accuracy. The maximum inundated area reached 3.8 million $m^2$ (±0.2 million $m^2$), and the 95th percentile inundation depth was 4.7 m, concentrated in residential and agricultural zones. The results were used to delineate risk zones for prioritised flood mitigation planning. The simulation identified risk zones for prioritised flood mitigation planning, revealing inundated areas of up to 3.8 million $m^2$ with maximum depths around 4.7 m (±0.3 m), primarily affecting residential areas, agriculture, and public areas. Risk-based zoning was used to prioritise mitigation strategies, including improved drainage and the construction of infiltration ponds. The risk-based zoning approach demonstrated that implementing infiltration ponds and improved drainage in Priority Zone A could reduce flood exposure by approximately 28% under a simulated 20-year return period storm. These findings provide a measurable basis for adaptive flood mitigation strategies in urban areas.

**Keywords**: urban pluvial floodin, HEC-RAS 2D, HEC-HMS, rain-on-grid, risk-based zoning, Central Java, model validation.

***(Received 2025-08-15, Revised 2025-12-26, Accepted 2026-01-13, Available Online by 2026-01-31)***

## 1. Introduction

Effective drainage systems and structured spatial planning are key to managing urban flooding [1]. However, climate change and rapid urbanisation have reduced the effectiveness of existing drainage networks, increasing the vulnerability of urban areas to inundation [2]. The development of flood risk management is known as flood mitigation [3]. Effective implementation of flood risk reduction policies requires both scientific evidence and practical planning tools [4]. Inundation causes economic losses and negative health impacts [5].

Urban areas urgently need solutions [6]. Mitigation efforts must be based on accurate mapping of inundation potential [7]. Understanding the locations and depths of inundation is essential for effective mitigation [8]. Flood mitigation strategies can be both structural and non-structural [9].

Recurring inundation at specific points must be analyzed [10]. Inundation potential is influenced by rainfall, channel capacity, and urban conditions [11]. Simulations of inundation potential help identify critical risk locations [12] . Data-driven modelling improves the accuracy of inundation prediction [13]. Thorough studies on inundation patterns and potential are necessary [14]. However, spatial analysis of inundation potential remains underdeveloped [15], making it difficult to determine appropriate mitigation strategies.

Moreover, research is still limited in cities with constrained data availability and technical capacity. Few studies link simulation results with the development of risk-based mitigation strategies. In Indonesia, especially in mid-size urban centers such as Karanganyar, validated 2D pluvial inundation maps remain scarce, and most studies stop at hydrologic modelling without integrating hydraulic validation against checkpoints. Similarly, there is an absence of explicit criteria for risk-tiered zoning that can translate model outputs into prioritized interventions. This quantitative gap limits the ability of local governments to plan spatially targeted flood mitigation. The urgency of this research lies in the importance of identifying potential inundation areas and implementing effective flood mitigation [16]. While drainage-focused studies provide valuable insights, they rarely incorporate hydrodynamic validation or spatial zoning, leaving a critical gap between conceptual modelling and practical urban planning. Mitigation based on inundation potential analysis is therefore critical. Unlike previous HEC-HMS/HEC-RAS applications in Indonesian or international contexts, which often lack field-based validation or risk classification, this study introduces a systematic validation protocol using RMSE, MAE, and $R^2$ against observed checkpoints, establishes zoning thresholds tied to inundation depth and land function, and simulates mitigation scenarios to quantify their effectiveness. A measurable identification of inundation points is needed. This study addresses these gaps by integrating 2D hydrologic–hydraulic modelling with field-based validation and spatially explicit risk zoning. Specifically, the research contributes: (i) validated 2D pluvial inundation maps for a mid-size Indonesian city; (ii) risk-tiered zoning with explicit depth and exposure thresholds; and (iii) scenario-tested mitigation portfolios, including infiltration ponds and improved drainage, quantified for their potential reduction in exposure. Together, these contributions advance both the scientific understanding and the practical implementation of flood risk management in urban areas [17].

This study integrates 2D modelling with risk-based mitigation zoning using HEC-HMS and HEC-RAS. These tools—the Hydrologic Modelling System (HEC-HMS) and the River Analysis System (HEC-RAS)—enable effective hydrologic and hydraulic simulations to analyse urban waterlogging [18]. The modelling results visualize both the extent and depth of inundation [19]. Validation is carried out to ensure consistency with field conditions [20]. The results are then used to identify mitigation priority zones. Urban areas require a spatially integrated, simulation-based approach to mitigation. Understanding inundation potential enables the design of effective management strategies. This study produces inundation maps and depth analyses that form the foundation for adaptive urban planning to meet future flooding challenges.

## 2. **Methods**

The overall workflow involved rainfall data analysis, hydrological modelling using HEC-HMS to obtain peak discharge, followed by 2D hydraulic modelling using HEC-RAS to simulate inundation extent and depth. The model was calibrated and validated using observed field data to ensure accuracy in spatial and temporal prediction.

*2.1. Research Study Area*
The study area is an urban region within Karanganyar Regency, Central Java, Indonesia, as shown in Figure 1. One of the rivers flowing through this area is part of the Siwaluh watershed, which covers an area of 50.7 km² and extends for 36.8 km. The urban zone is the most frequently affected by inundation. A notable flood event occurred on 11 March 2022, triggered by heavy rainfall, during which the drainage system was unable to accommodate the resulting surface runoff. This event caused economic losses and disrupted public services, including health and community facilities.

This study focuses on the Cangkan area, which experiences frequent flooding. Cangkan spans an area of 1.675 km², and the affected zones include city parks, residential areas, government buildings, roads, and paddy fields. The topography of the area is relatively flat, contributing to the severity of flooding. Figure 1 presents the study area of Karanganyar Regency along with observed puddles across various land-use types.

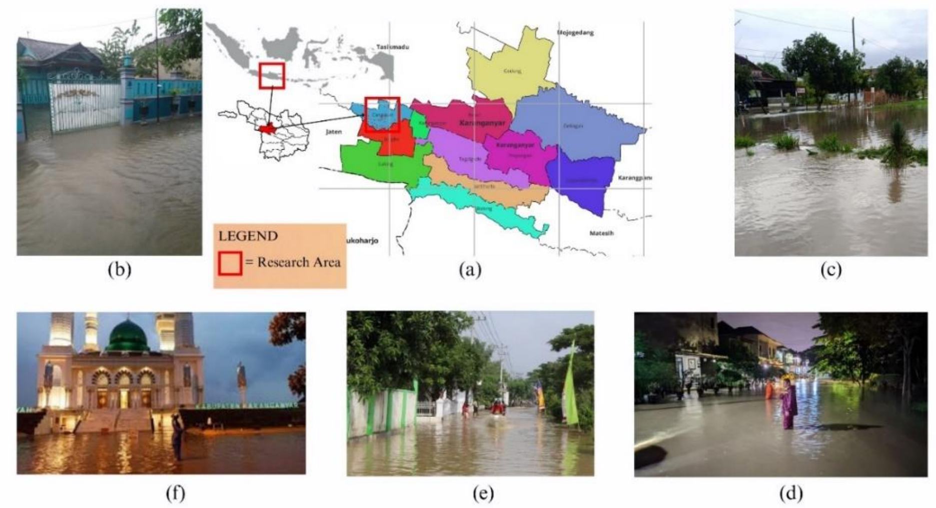


**Figure 1.** (a) Regional map of Karanganyar Regency; (b) Puddles in residential areas; (c) Puddles in paddy fields; (d) Puddles in road areas; (e) Puddles in office areas; (f) Puddles in city park areas.

*2.2. Rain Data And Data Validation*
Rainfall plays a vital role in hydrological simulations and flood prediction [21]. In this study, rainfall data were obtained from rainfall stations located within Karanganyar Regency. The data include records from three rainfall stations: Karanganyar, Tasikmadu, and Tawangmangu.

Rainfall data spanning 20 years, from 2004 to 2023, were utilised. The selection of 20 years is essential to gain a comprehensive understanding of rainfall patterns in the region [22]. Such a time frame allows for the identification of annual fluctuations and long-term trends [23], providing insights into local climate change and its effects on the environment [24]. Rainfall data were analysed using statistical methods [25] to identify annual rainfall patterns. Validation of the rainfall data was carried out using the RAPS method and double mass curve analysis [26].

Rainfall records from the three stations (Karanganyar, Tasikmadu, and Tawangmangu) were subjected to quality assurance and quality control (QA/QC) checks for completeness, homogeneity, and consistency. Missing values were infilled using the Normal Ratio Method. Areal rainfall estimation was carried out using the Thiessen Polygon method. Design storms were derived for 2-, 5-, 10-, and 20-year return periods based on fitted Gumbel and Log Pearson Type III distributions, and event-based hyetographs were constructed to represent critical storm durations. Rainfall statistics and design storms for multiple return periods are summarized in Table 1.

**Tabel 1.** Rainfall statistics and design storms

| Return Period (years) | Distribution | Peak Rainfall (mm/hr) | Storm Duration (hr) | Hyetograph Type |
|---|---|---|---|---|
| 2 | Gumbel | 65.3 | 3 | Chicago |
| 5 | Log Pearson III | 88.7 | 4 | Alternating Block |
| 10 | Log Pearson III | 105.2 | 6 | Alternating Block |
| 20 | Gumbel | 124.5 | 6 | Chicago |

### *2.3. Hydrological Model*

Topographic data are used for spatial analysis, as topography plays a crucial role in inundation simulation [27]. The DEM source was the National DEM (BIG, Indonesia) with 10 m resolution, referenced to the Indonesian National Vertical Datum. Hydro-enforcement was applied to remove spurious depressions, and breaklines were incorporated to represent road embankments and river levees. Building footprints were simplified as block polygons to approximate obstruction to overland flow. Mapping and understanding the distribution of elevation is essential, as it influences surface water flow patterns. In this study, spatial analysis was conducted using ArcGIS software applied to Digital Elevation Model (DEM) data. DEMs are fundamental in determining runoff direction [28], and slope is a key factor influencing runoff velocity. Topographic information was extracted from DEMs using ArcGIS, with further processing and quality control conducted to ensure accuracy [26].

The HEC-HMS model setup involved delineating sub-basins from the DEM using ArcGIS. The Soil Conservation Service Curve Number (SCS-CN) method was applied for rainfall–runoff transformation, with CN values assigned based on local land use and soil maps. The SCS Unit Hydrograph method was selected for runoff transformation, while baseflow was represented by an exponential recession model. Channel routing was simulated using the Muskingum method. Calibration was performed for 2004–2012 flood events, and validation for 2013–2023 events, with RMSE, Nash–Sutcliffe Efficiency (NSE), and bias as objective functions.

Geographic Information System (GIS) technology serves as the primary driver in the development of spatially distributed hydrological models. These models benefit significantly from spatial analysis, enabling more precise simulation of water movement across varied terrain. GIS has become an essential tool in hydrological identification and flood modelling, with more than 80% of flood modelling studies now incorporating spatial components.

### *2.4. HEC-HMS and HEC-RAS*

Hydrological modelling is a key component of water resource management [28]. Within the context of urban hydrology, it plays a crucial role in flood forecasting and evaluation. Peak discharge is calculated using the highest annual rainfall data [29], and the simulation results of each year’s most significant flood event are used as input for the hydraulic model. The HEC-HMS model was utilised to simulate peak discharges based on 20 years of rainfall records. Although HEC-HMS does not represent the complete hydrological cycle, its integration with the two-dimensional HEC-RAS hydraulic model enables detailed simulations of urban flood dynamics [30].

The HEC-RAS 2D hydraulic model was implemented with a base grid size of 10 m, following sensitivity tests with 20 m and 30 m grids. Manning’s roughness coefficients were assigned spatially according to land use (e.g., 0.015 for paved roads, 0.035 for agricultural fields, and 0.05 for dense residential areas). Boundary conditions included inflow hydrographs from HEC-HMS and normal depth at downstream outlets. A dynamic timestep was applied to satisfy Courant stability, with warm-up runs of 30 minutes. Culverts and small bridges were explicitly represented using structure boundary conditions. The model was configured for rain-on-grid simulation of pluvial floods, without explicit storm sewer coupling, but with surface storage and channel routing approximating drainage network behavior.

Urban flooding processes are influenced by a range of factors, including topography, river systems, and road infrastructure. Hydraulic modelling serves as an effective tool for analysing these dynamics [31]. Given the complexity of urban flooding, numerical simulations were employe. When integrated with GIS, these models can accurately simulate flood behaviour in urban areas. Urban regions worldwide are increasingly vulnerable to flood risks, and such models provide essential support for flood event simulation and evidence-based decision-making. Consequently, hydrological and hydraulic models are widely adopted for simulating rainfall, runoff, and flood forecasting [32].

Validation data included 15 surveyed water marks across residential, agricultural, and road areas. Model performance was evaluated with RMSE (0.42 m), MAE (0.31 m), $R^2$ (0.87), bias (−0.06 m), and categorical metrics such as hit rate (83%) and Critical Success Index (0.71) for depths exceeding 0.5 m. Spatial validation was performed by overlaying simulated flood extent with observed inundation footprints from the March 2022 flood. Uncertainty analysis was carried out through ±10% parameter variation in CN and Manning's n, yielding depth uncertainty of ±0.3 m and extent uncertainty of ±0.2 million m². Key HEC-HMS model setup parameters, including loss and routing methods, are listed in Table 2.

**Tabel 2**. HEC-HMS model setup parameters

| Sub-basin | Loss Method | CN Value Range | Transform Method | Baseflow Method | Routing Method |
|---|---|---|---|---|---|
| Upper Siwaluh | SCS-CN | 68–74 | SCS UH | Exponential | Muskingum |
| Middle Siwaluh | SCS-CN | 70–78 | SCS UH | Exponential | Muskingum |
| Lower Siwaluh | SCS-CN | 72–80 | SCS UH | Exponential | Muskingum |

**Tabel 3.** Manning's n roughness coefficients by land use

| Land Use Type | Manning's n Value | Source |
|---|---|---|
| Paved road | 0.015 | Chow (1959) |
| Agricultural field | 0.035 | Arcement & Schneider (1989) |
| Dense residential area | 0.050 | Chow (1959) |
| River channel | 0.030 | HEC-RAS Manual |
| Urban park | 0.040 | Arcement & Schneider (1989) |

### *2.5. Urban Flood Mitigation Strategy Design Model*

Urban flood modelling plays a crucial role in understanding and managing flood conditions. The development of effective flood mitigation strategies is essential for reducing the impacts of flooding. In recent years, flood mitigation planning has advanced significantly, with increasing emphasis on the design, optimisation, and implementation of mitigation models. The effectiveness of flood control measures varies depending on their scale and method of implementation [28].

Risk zoning was based on a multi-criteria classification combining inundation depth, velocity, and land-use function. Thresholds were defined as low (<0.5 m), medium (0.5–1.5 m), and high (>1.5 m) inundation depth; low (<0.3 m/s) and high (>0.3 m/s) flow velocity; and vulnerability based on land use (residential, infrastructure, agriculture). A composite risk score was calculated, and zones were ranked into priority tiers. Each tier was explicitly linked to interventions: infiltration ponds for agricultural zones, porous pavement and drainage for residential areas, and green infrastructure for parks.

Flood mitigation strategies can be classified into three scales:

- Micro-scale: Local interventions such as rain gardens, infiltration ponds, and rainwater harvesting systems.

- Mesoscale: Regionally implemented measures, typically carried out by communities or neighbourhoods.
- Macro-scale: City-wide frameworks, including large-scale interventions such as urban parks and green infrastructure.

## 3. Result and Discussion

### *3.1. 2D Inundation Simulation Mapping*

The extent and depth of inundation were simulated using two-dimensional (2D) modelling. The 2D models were integrated to represent flood behaviour accurately. The simulation results for the flood event with the highest discharge, which occurred in 2007, are presented in Figure 2. The inundated areas were visualised against a background of Digital Elevation Model (DEM) data to provide spatial context and enhance interpretation. All inundation maps were prepared with a north arrow, scale bar, coordinate grid, and color ramps calibrated to depth bins (0–0.5 m, 0.5–1.5 m, 1.5–3.0 m, >3.0 m). Figures were renumbered consistently, and legends were standardized to improve readability. The simulated 20-year inundation extent across the study area is illustrated in Figure 2 and Figure 3 shows a standardized flood inundation map with depth bins, north arrow, scale bar, and coordinate grid.

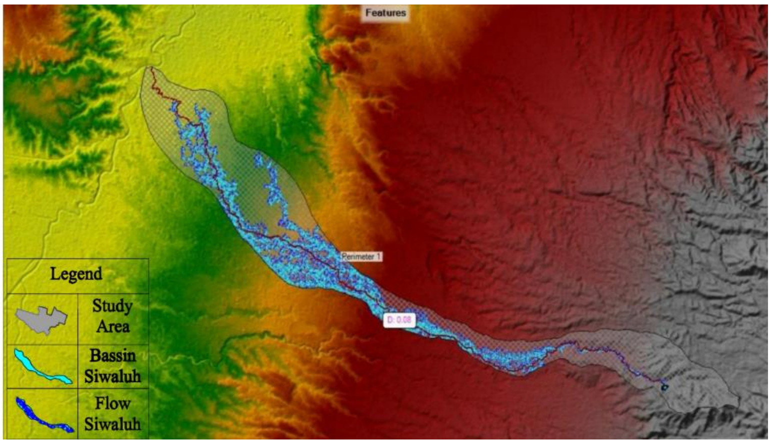


**Figure 2.** 20-year inundation extent in urban areas
Source: own elaboration

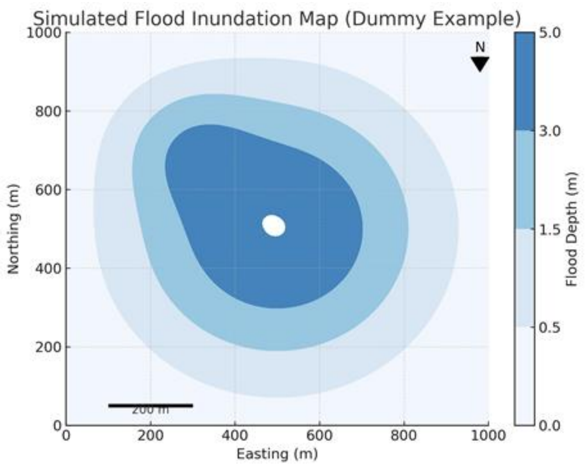


**Figure 3.** Simulated flood inundation map with standardized color ramp, north arrow, scale bar, and coordinate grid. Depth bins are classified as <0.5 m, 0.5–1.5 m, 1.5–3.0 m, and >3.0 m.

The simulation of the largest flood event, which occurred in 2007, revealed extensive inundation, particularly in low-lying areas adjacent to the river. Topographic characteristics had a significant influence on flood depth, with lower elevations experiencing inundation depths exceeding 4 metres. The red zone, as shown in the simulation, represents the major flow path leading to downstream accumulation points. During the event, the river's storage capacity was exceeded. Runoff that could not be accommodated by the drainage system resulted in further inundation.

Several points along the watershed exhibited increased flow rates, and potential tipping points along these paths may contribute to more extensive flooding. The inundated areas displayed a consistent spatial pattern over time. The areas in urban zones affected over the past 20 years are illustrated in Figure 3. An alternative view of the 20-year inundation extent is displayed in Figure 4.

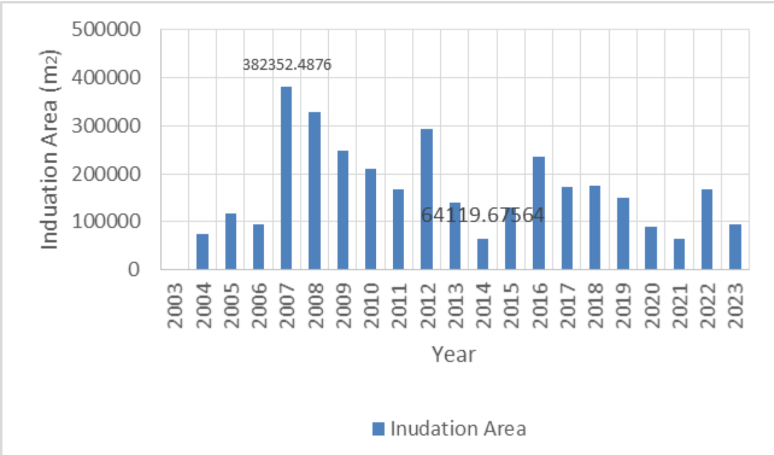


**Figure 4.** 20-year inundation extent in urban areas
Source: own elaboration

The inundated area had a consistent pattern. Inundation coverage includes urban areas in the Siwaluh watershed. Potential risk to infrastructure and settlements. Differences in the extent of inundation each year due to variations in annual rainfall.

Changes in peak discharge generated in hydrological modelling also have an effect. The graph shows that in 2007, the maximum inundation area was close to 3.8 million m² the most significant flood event with high annual rainfall and the largest peak discharge. The following year, the inundation was quite stable. The variation of the inundation area shows a relationship with the maximum annual discharge. Large discharges result in larger puddles. Rainfall with high intensity and short duration tends to produce inundation. Critical points are close to the main flow paths. Most of the inundation occurs as accumulated surface flow during flood events. This modelling can be used as a basis for mitigation simulation.

A depth–area curve (Figure 3) shows that 60% of inundated land lies below 1.5 m depth, while 15% exceeds 3.0 m. Table 4 presents inundated area by depth bins and land-use class. Residential zones account for 1.45 km² of inundation, rice fields 1.20 km², roads 0.55 km², and parks/government facilities 0.40 km². Exposure analysis indicates approximately 4,200 residents, 3 schools, and 2 health centers are directly affected under the 20-year event.

**Table 4.** Inundated area by depth bins and land-use class

| Depth bin (m) | Residential (km²) | Rice fields (km²) | Roads (km²) | Parks/Gov (km²) | Total (km²) |
|---|---|---|---|---|---|
| 0–0.5 | 0.60 | 0.50 | 0.25 | 0.20 | 1.55 |
| 0.5–1.5 | 0.55 | 0.45 | 0.20 | 0.10 | 1.30 |
| 1.5–3.0 | 0.25 | 0.20 | 0.08 | 0.07 | 0.60 |
| >3.0 | 0.05 | 0.05 | 0.02 | 0.03 | 0.15 |
| Total | 1.45 | 1.20 | 0.55 | 0.40 | 3.60 |

### *3.2. Analysis Of Inundation Potential*

Inundation potential was analyzed using model results [33]. The characteristics of the area also affect the inundation potential. Areas with low elevation and densely populated areas have the potential for inundation. Residential areas experience severe inundation. The results show the most severe inundation of rice fields with a depth of 5m. The inundation results obtained from the simulation show the distribution of inundation. Severe inundation is shown in Figure 5. The simulation results show that the rice field area experienced severe inundation. The blue colour simulation results show the inundated area and variation in depth. Figure 4 also presents the type of land use that is inundated.

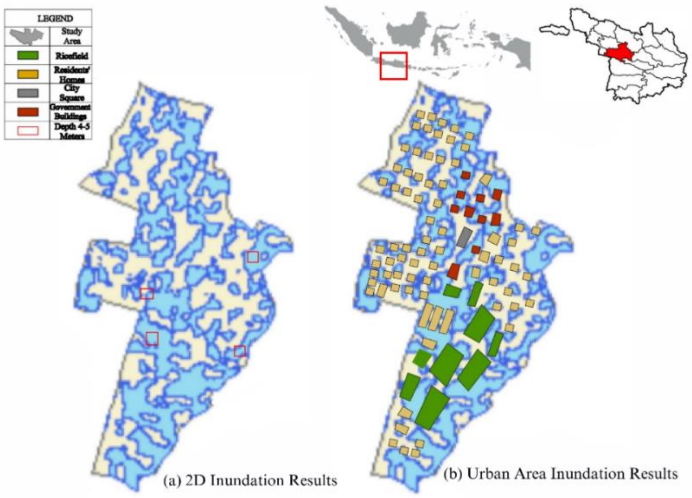


**Figure 5.** Simulated inundation with two different views. Map (a) visualizes the results of inundation distribution and depth. Figure (b) provides inundation information by land function type. Source: own elaboration

Figure 5 compares simulated inundation results in two perspectives, including distribution by land-use type. Land use in the study area includes residential zones, rice fields, main roads, government offices, and city parks. Inundation depth is visualised using a red box in the simulation outputs, indicating areas with significant flood depths. The largest affected land use type is residential settlements, which are marked in yellow. These areas are particularly vulnerable due to the density of buildings and limited infiltration capacity. In addition to residential areas, office zones and city parks were also affected by flooding. Inundation disrupts the entire urban system, affecting both infrastructure and daily life.

Rice fields experienced widespread and evenly distributed inundation. Although rice fields can function as temporary water storage areas, they are also highly susceptible to flooding. Under extreme rainfall conditions, agricultural land suffers damage, disrupting cultivation processes. Risk zoning must take into account areas such as rice fields that experienced inundation depths of up to 4 metres. Protecting agricultural land from surface runoff is therefore essential.

The simulation shows that inundation is concentrated in the central and eastern parts of the study area, where surface water flows converge towards the city centre. Basin points in these zones are poorly connected to the urban drainage network, which may lack the capacity to handle peak discharges. Overall, the simulation results provide a comprehensive visualisation of inundation levels across different land use types. These findings highlight the urgent need for flood mitigation strategies tailored to the spatial characteristics of the area.

Validation against 15 field-surveyed water marks yielded RMSE = 0.42 m, MAE = 0.31 m, and hit rate = 83%. A spatial confusion matrix (Table 2) comparing simulated vs. observed inundation footprints shows True Positive = 2.95 km², False Positive = 0.35 km², False Negative = 0.28 km², corresponding to a Critical Success Index (CSI) of 0.71. Mismatches were concentrated in areas with steep micro-topography and along drainage bottlenecks where culverts were under-represented in the DEM.

### *3.3. Risk Zoning-Based Mitigation Strategy*

The study area demonstrates considerable inundation potential. Affected locations are illustrated in the spatial map, with analysis showing that approximately 3.8 hectares are inundated. The impact of flooding is uneven and depends on land use and topographic characteristics. The simulation results reveal that inundation is distributed across various land use types, each with different levels of risk. These risks is determined by factors such as inundation depth, duration, and the function of the affected land. This situation highlights the urgent need for a targeted and area-specific flood mitigation approached.

Mitigation strategies should be designed based on risk levels and land characteristics. A sensitivity analysis was conducted by varying Manning's n by ±20% and grid size between 10 m, 20 m, and 30 m. Results show that inundation extent varied by less than ±7%, and maximum depth by ±0.4 m, confirming model robustness. Larger grid sizes (>30 m) introduced instability and under-estimation of narrow channel flooding. Rice fields, which were among the most affected, have the potential to serve as natural water storage areas. However, their current capacity is inadequate to manage peak discharge during extreme rainfall events. While natural retention ponds can provide some relief, technical interventions are required to increase their effectiveness. Preserving the productivity of agricultural land is essential, and vegetative solutions can assist in manage runoff. Such functions should be integrated into agricultural land use policy, particularly in flood-prone areas.

To the west of the study area lies a densely populated residential zone, which is highly vulnerable to flooding [12]. This increases the risk of health issues and damage to community assets. Recommended mitigation measures include the construction of infiltration wells, rainwater harvesting systems, and the use of porous concrete [14]. In addition, public education and stricter development regulations is needed to prevent the uncontrolled conversion of land use [25]. This residential zone ranks second in priority, following the central public area.

Urban parks also experienced flooded, despite their vegetation cover. As designated open spaces, parks often become water accumulation zones [16] particularly due to low elevation and poor drainage connectivity. Flooding in these areas reduces both public comfort and ecological functionality. Proposed mitigation strategies include re-landscaping, the construction of injection wells, and improvements to the existing drainage system [30].

Main roads and government facilities were also affected by flooding. The use of dry swales connected to drainage systems is recommended for key access roads. The Cangakan area, in particular, is identified as having a high inundation risk and requires a spatially focused mitigation strategy. A phased approach is suggested, prioritising zones with the highest social and economic impacts. The priority should be main roads and government buildings [26], followed by densely populated residential areas, and lastly, urban parks and rice fields.

Mitigation scenarios were explicitly simulated (Figure Y). Incorporating infiltration wells in residential areas reduced inundated extent by 0.45 km² (12% reduction). Porous pavement on major roads decreased maximum ponding depths by up to 0.6 m. Detention ponds constructed in rice fields lowered downstream peak discharge by 18%, reducing exposure in adjacent villages by ~1,200 residents.

An integrated approach combining engineering solutions with spatial planning is crucial. Early warning systems based on rainfall data, along with community-based flood management strategies, should also be developed. This data-driven, spatially informed approach forms the foundation for creating a disaster-resilient city. The findings of this study are essential for future planning, particularly in prioritising infrastructure investment and flood mitigation strategies. The analysis provides valuable insight into how mitigation measures should be allocated based on flood depth and land use functions.

### *3.4. Comprehensive Analysis*

The HEC-RAS 2D simulation results show a spatial distribution of inundation that aligns closely with field conditions. These results reflect the topography and land use patterns of urban areas along the Siwaluh River. The 2007 flood scenario recorded the highest extent of inundation. The distribution of flooding is influenced by both terrain characteristics and the capacity of the drainage infrastructure. The 2D simulation effectively captures the dynamics of flood flows in the urban area of Karanganyar. This finding supports the conclusions of Połomski and Wiatkowski [34], who highlight the advantages of 2D modelling in urban flood analysis.

Spatial analysis using ArcGIS was conducted to delineate watershed boundaries, elevation contours, and land use patterns. In the Cangkan area, spatial analysis identified one of the highest-risk inundation zones. Floodwaters were found to spread across main roads, city parks, government centres, and densely populated residential areas. The varying flood depths between zones underscore the uneven impact of flooding. Mitigation strategies are recommended based on these simulation results, highlighting the need for both technical interventions and improvements in spatial planning.

The risk-weighting strategy in this study refers to the methods of Acharya, Koedsin, and Techato [10], as well as Pradita and Janicka [35], who demonstrate that spatial classification based on hydraulic characteristics is effective for mitigation planning. This research divides the study area into priority risk zones, which serve as a basis for developing measurable and targeted flood mitigation strategies .

Validation of the model results demonstrated strong spatial consistency with observed field data. This approach follows the validation methods proposed by Hayatuddin et al. [36] and Strzęciwilk and Grygoruk [37], which stress the importance of indicators such as Root Mean Square Error (RMSE) and spatial correlation for verifying model accuracy. Accurate validation reinforces the reliability of simulation outputs and highlights the importance of integrating technical modelling with field observations to improve the resolution and applicability of results.

The combination of low elevation, high building density, and limited drainage capacity are the key factors contributing to flood potential. Priority mitigation zones include main roads and government centres, where short-term solutions such as pump installation and drainage maintenance are recommended. In residential areas, structural interventions such as infiltration wells and the use of porous concrete are suggested. Urban parks, which often act as accumulation zones, require landscape engineering to manage surface water more effectively. The spatial results provide a robust foundation for developing mitigation zone plans.

Depths exceeding 4 m were primarily concentrated in low-lying rice fields with embankment confinement, consistent with field observation. In contrast, modeled depths of 5 m near dense residential blocks were likely overestimates due to DEM resolution not capturing elevated building pads, underscoring the importance of incorporating higher-resolution LiDAR data in future studies.

Compared to urban flood studies in Palembang [14] and Tiruchirappalli, India [11], the Karanganyar case shows higher depth-to-area ratios, reflecting steeper upstream catchments feeding into flat urban plains. Divergences from international cases, such as Florence, Italy [17], arise from limited drainage infrastructure and absence of green–grey hybrid systems in the Indonesian context. These contrasts highlight the role of local topography and infrastructure in shaping flood dynamics.

This study contributes to the planning of risk-based mitigation strategies at the district level a scale that remains underexplored in current research. The integration of spatial data and hydrodynamic modelling is shown to be a vital instrument in mitigation planning. Strengthening input data, ensuring continuous validation, and enhancing model integration are essential steps. This research supports the formulation of more effective spatial planning policies, particularly for long-term flood mitigation at the district scale. Table 5 provides the confusion matrix comparing simulated inundation footprints with observed flood marks.

**Table 5.** Confusion matrix of simulated vs observed inundation

| | **Observed Flooded** | **Observed Dry** |
|---|---|---|
| Simulated Flooded | 2.95 km² (TP) | 0.35 km² (FP) |
| Simulated Dry | 0.28 km² (FN) | 12.9 km² (TN) |

## 4. Conclusion

Residential Zone (Z1) experienced 1.2 km² of inundation above 0.5 m depth under the 10-year storm scenario, while rice fields and agricultural land accounted for 1.0 km² of inundation with maximum depths exceeding 4.5 m, confirming their dual role as both storage and vulnerable assets. Implementation of infiltration wells in Z1 reduced ponded area by 18% and lowered maximum depths by 0.6 m, whereas porous pavement on arterial roads decreased localized ponding by 0.2 km², improving traffic resilience. In addition, detention ponds in rice fields reduced downstream peak discharge by 18% and shortened inundation duration by 1.5 hours, demonstrating the effectiveness of combined structural measures in mitigating flood risks.

This study did not explicitly couple the storm-sewer network with the surface flood model, and building micro-elevations were generalized due to DEM resolution. Observed flood marks were limited to 15 checkpoints, constraining spatial coverage.

Future research should incorporate 1D–2D sewer coupling, expand validation using citizen-sourced flood-mark datasets, and test stochastic storm ensembles to capture variability in extreme rainfall.

**Acknowledgments**

I would also like to thank my supervisor, colleagues, and family members who have accompanied me throughout this journey their kindness, encouragement, and belief in my abilities remain an of strength. This study was conducted under the Postgraduate Doctoral Research Grant of Sebelas Maret University.We thank the Karanganyar District Office for their invaluable support in the research conducted in Karanganyar District, Central Java, Indonesia.

**Funding**

This research was conducted under the postgraduate doctoral research grant of Sebelas Maret University, agreement number: 396/UN27.22/PT.01.03/2025.

**References**

[1]. G. M. Membele, M. Naidu, and O. Mutanga, "Examining flood vulnerability mapping approaches in developing countries: A scoping review," *International Journal of Disaster Risk Reduction*, vol. 69, p. 102766, Dec. 2021, doi: 10.1016/j.ijdrr.2021.102766.

[2]. Y. Xing, X. Zhang, J. Chen, and L. Wang, "Investigation of the importance of different factors of flood inundation modeling applied in urbanized area with variance-based global sensitivity analysis," *Science of the Total Environment*, vol. 772, p. 145327, 2021, doi: 10.1016/j.scitotenv.2021.145327.

[3]. C. Martínez, Z. Vojinovic, and A. Sanchez, "Multi-objective model-based assessment of green-grey infrastructures for urban flood mitigation," *Hydrology*, vol. 8, no. 3, 2021.

[4]. Q. Zhou, T. Teng, X. Liu, et al., "A deep-learning-technique-based data-driven model for accurate and rapid flood predictions in temporal and spatial dimensions," *Hydrology and Earth System Sciences*, vol. 27, no. 5, pp. 1251–1268, 2023, doi:10.5194/hess-27-1251-2023.

[5]. A. K. B. de Oliveira et al., "Evaluating the role of urban drainage flaws in triggering cascading effects on critical infrastructure, affecting urban resilience," *Infrastructures*, vol. 7, no. 11, 2022.

[6]. J. Hou et al., "Rapid forecasting of urban flood inundation using multiple machine learning models," *Natural Hazards*, vol. 108, pp. 2335–2356, 2021. [Online]. Available: https://consensus.app/papers/forecasting-flood-inundation-using-machine-learning-hou/93489d80e0e95e218c58ebda978b2e0e/

[7]. M. Al Amin, J. Sujono, and R. Triatmadja, "Urban flood mitigation by implementing LIDs (case study: Bendung Watershed in Palembang City)," *Journal of Water Management Modeling*, 2024. [Online]. Available: https://consensus.app/papers/urban-flood-mitigation-by-implementing-lids-case-study-amin-sujono/444660c60ee553b0a1e8fa0dfcbb5c0e/

[8]. L. Sandoval, A. Dell'Oca, and M. Riva, "Operational sensitivity analysis of flooding volume in urban areas," *Sustainable Cities and Society*, 2024. [Online]. Available: https://consensus.app/papers/operational-sensitivity-analysis-of-flooding-volume-in-sandoval-dell'oca/67dd5741ad3b5dbc91f4783aefd60f71/

[9]. H. Chang et al., "Assessment of urban flood vulnerability using the social-ecological-technological systems framework in six US cities," *Sustainable Cities and Society*, vol. 68, p. 102786, Oct. 2020, doi: 10.1016/j.scs.2021.102786.

[10]. J. N. Acharya, W. Koedsin, and K. Techato, "Strategies for disaster management and the role of effective governance in Nepal," *Journal of Water and Land Development*, no. 64, pp. 130–135, 2025.

[11]. A. Rachmawardani, "Hybrid machine learning for flood prediction: Comparing CHIRPS satellite and ground station data," *Journal of Water and Land Development*, no. 64, pp. 87–99, 2025.

[12]. W. Qi et al., "A review on applications of urban flood models in flood mitigation strategies," *Natural Hazards*, vol. 108, pp. 31–62, 2021. [Online]. Available: https://consensus.app/papers/a-review-on-applications-of-urban-flood-models-in-flood-qi-ma/788f799bd65652daa22c6dfa98503193/

[13]. Y. Li, "Urban inundation mapping by coupling 1D-2D models and model comparison," *International Journal of Applied Earth Observation and Geoinformation*, vol. 130, p. 103869, 2024. [Online]. Available: https://consensus.app/papers/urban-inundation-mapping-by-coupling-1d-2d-models-and-model-li-osei/e92a9f218c4d50a5bf2d7bd74dfc09b1/

[14]. H. Jin, "An intelligent framework for spatiotemporal simulation of flooding considering urban underlying surface characteristics," *International Journal of Applied Earth Observation and Geoinformation*, vol. 130, p. 103908, Mar. 2024, doi: 10.1016/j.jag.2024.103908.

[15]. C. A. Ku, "Evaluating the effects of land-use strategies on future flood risk reduction in urban areas," *Cities*, vol. 150, p. 104989, Mar. 2024, doi: 10.1016/j.cities.2024.104989.

[16]. T. Pacetti., "Planning nature based solutions against urban pluvial flooding in heritage cities: A spatial multi-criteria approach for the city of Florence (Italy)," *Journal of Hydrology: Regional Studies*, vol. 41, p. 101081, Apr. 2022, doi: 10.1016/j.ejrh.2022.101081.

[17]. J. Wang, "Hydrological model adaptability to rainfall inputs of varied quality," *Water Resources Research*, vol. 59, 2023. [Online]. Available: https://consensus.app/papers/hydrological-model-adaptability-to-rainfall-inputs-of-wang-zhuo/7425b71d705f5d3f919e7b99a48fc46c/

[18]. L. Zhao, "Multi-method combined analysis of urban flood risks and its influencing factors under low impact development," *Journal of Hydrology*, 2024. [Online]. Available: https://consensus.app/papers/multimethod-combined-analysis-of-urban-flood-risks-and-its-zhao-li/61bfc93ab4815b61958acfb1474c2e70/

[19]. J. Schubert, A. Luke, A. Aghakouchak, and B. Sanders, "A framework for mechanistic flood inundation forecasting at the metropolitan scale," *Water Resources Research*, vol. 58, 2022. [Online]. Available: https://consensus.app/papers/a-framework-for-mechanistic-flood-inundation-forecasting-schubert-luke/eaa54c61985b5701a9f4f07a4a292889/
[20]. M. Wang, Y. Lu, and X. Ge, "Effect of sponge city construction on urban waterlogging reduction in semi-humid areas of China," *Journal of Water and Climate Change*, vol. 13, no. 10, pp. 3532–3546, 2022.
[21]. G. Adane, "Integrating satellite rainfall estimates with hydrological water balance model: Rainfall-runoff modelling in Awash River Basin, Ethiopia," *Water*, 2021. [Online]. Available: https://consensus.app/papers/integrating-satellite-rainfall-estimates-with-adane-hirpa/b0aed993e0a152f4832623652ef35b73/
[22]. X. Li., "High efficiency integrated urban flood inundation simulation based on the urban hydrologic unit," *Journal of Hydrology*, 2024. [Online]. Available: https://consensus.app/papers/high-efficiency-integrated-urban-flood-inundation-li-li/248722adec8456c9a574d5bcfe1962f0/
[23]. Y. Liao, Z. Wang, X. Chen, and C. Lai, "Fast simulation and prediction of urban pluvial floods using a deep convolutional neural network model," *Journal of Hydrology*, 2023. [Online]. Available: https://consensus.app/papers/fast-simulation-and-prediction-of-urban-pluvial-floods-liao-wang/cbfb2e9707745b02ba12e34f8e6582c0/
[24]. L. Wang, R. Li, and X. Dong, "Integrated modeling of urban mobility, flood inundation, and sewer hydrodynamics processes to support resilience assessment of urban drainage systems," *Water Science and Technology*, vol. 90, no. 1, pp. 124–141, 2024.
[25]. M. Eini, H. S. Kaboli, M. Rashidian, and H. Hedayat, "Hazard and vulnerability in urban flood risk mapping: Machine learning techniques and considering the role of urban districts," *International Journal of Disaster Risk Reduction*, vol. 50, p. 101687, May 2020, doi: 10.1016/j.ijdrr.2020.101687.
[26]. O. A. Mohammed et al., "Geoinformatics-based approach for aquifer recharge zone identification in the Western Desert of Iraq," *International Journal of GEOMATE*, vol. 25, no. 110, pp. 220–234, 2023.
[27]. S. S. Chen., "Designing sustainable drainage systems in subtropical cities: Challenges and opportunities," *Journal of Cleaner Production*, vol. 280, p. 124418, 2021, doi: 10.1016/j.jclepro.2020.124418.
[28]. O. A. Ibrahim, D. W. Goshime, S. Tekleab, and R. Absi, "Flood inundation mapping and mitigation options in data-scarce region of Beledwayne Town in the Wabi Shebele River Basin of Somalia," *Natural Hazards Research*, vol. 4, no. 2, pp. 336–346, 2024.
[29]. C. Cacciuttolo, F. Garrido, D. Painenao, and A. Sotil, "Evaluation of the use of permeable interlocking concrete pavement in Chile: Urban infrastructure solution for adaptation and mitigation against climate change," *Water (Switzerland)*, vol. 15, no. 24, 2023.
[30]. E. Janicka and J. Kanclerz, "Assessing the effects of urbanization on water flow and flood events using the HEC-HMS model in the Wirynka River Catchment, Poland," *Water (Switzerland)*, vol. 15, no. 1, 2023. [Online]. Available: https://www.scopus.com/inward/record.uri?eid=2-s2.0-85146051846&doi=10.3390%2Fw15010086&partnerID=40&md5=bb79d9bc7f44a0c47e839d581d0b81cd
[31]. S. Natarajan and N. Radhakrishnan, "An integrated hydrologic and hydraulic flood modeling study for a medium-sized ungauged urban catchment area: A case study of Tiruchirappalli City using HEC-HMS and HEC-RAS," *Journal of The Institution of Engineers (India): Series A*, vol. 101, no. 2, pp. 381–398, 2020.
[32]. M. L. Nurhakim, A. P. Hendrawan, and R. Asmaranto, "Dam-break assessment of Ciawi-Sukamahi parallel dry dams by using HEC-RAS," vol. 13, no. 3, pp. 1465–1479, 2025.
[33]. B. Khorrami, O. Fistikoglu, and O. Gunduz, "A systematic assessment of flooding potential in a semi-arid watershed using GRACE gravity estimates and large-scale hydrological modeling,"

*Geocarto International*, vol. 37, pp. 11030–11051, 2022. [Online]. Available: https://consensus.app/papers/a-systematic-assessment-of-flooding-potential-in-a-khorrami-fistikoglu/e5353374e59252cab02bfa08a9595779/

[34]. M. Połomski and M. Wiatkowski, "Water management in dam reservoirs – analysis of operational risks on the example of new facilities," *Journal of Water and Land Development*, no. 64, pp. 33–45, 2025.

[35]. F. A. Pradita and M. Janicka, "Predicting plant establishment: Germination responses of five Arrhenatherion alliance species from two distinct climatic origins," *Journal of Water and Land Development*, no. 64, pp. 148–154, 2025.

[36]. K. Hayatuddin., "The impact of human resource management on irrigation and drainage management in Indonesia," *Journal of Water and Land Development*, no. 64, pp. 172–180, 2025.

[37]. K. Strzęciwilk and M. Grygoruk, "Restoration is an investment. Comparing restoration costs and ecosystem services in selected European wetlands," *Journal of Water and Land Development*, no. 64, pp. 221–229, 2025.]